Geo-information Science and Remote Sensing

Thesis Report GIRS-2019-38

Understanding crown shyness from a 3D perspective

Jens van der Zee

October 7, 2019

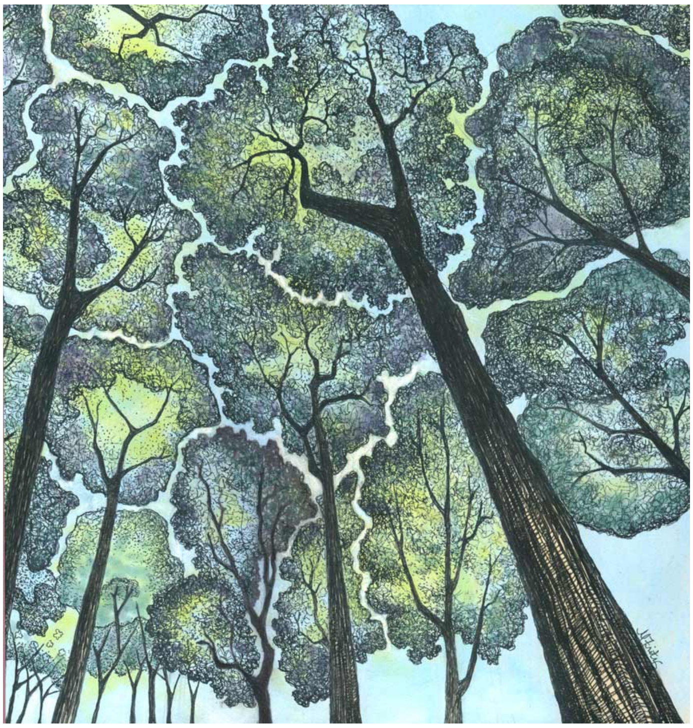

Artwork by Michele Fritz

WAGENINGEN
UNIVERSITY & RESEARCH

Understanding crown shyness from a 3D perspective

Jens van der Zee

Registration number 94 08 22 984 010

Supervisors:

Dr. Alvaro Lau (Wageningen University)
Dr. Alexander Shenkin (University of Oxford)

A thesis submitted in partial fulfilment of the degree of Master of Science
at Wageningen University and Research Centre,
The Netherlands.

October 7, 2019
Wageningen, The Netherlands

Thesis code number: GRS-80436
Thesis Report: GIRS-2019-38
Wageningen University and Research Centre
Laboratory of Geo-Information Science and Remote Sensing

Acknowledgements

I wish to express my gratitude to all the people that helped me to complete this thesis. I thank Benjamin Brede for inviting me to my first tropical field work experience to help with the collection of the data used in this thesis. The fieldwork would have been impossible without the people of the Guyana Forestry Commission who received us with open arms and worked hard to make the campaign a success.

I would like to thank Jan den Ouden whose lectures and thesis supervision during my BSc sparked my interest in forest ecology. Many thanks to Alexander Shenkin for providing me with useful insight on tree crown dynamics and motivating me with his contagious enthusiasm. My main supervisor, Alvaro Lau, has been incredibly accommodating throughout the entire process of writing this thesis. Thank you so much for coming up with the thesis topic, the joyful company during field work and sharing your office with me. Your guidance has been instrumental and I will be forever grateful to you for everything I have learned from completing this thesis.

Finally, I wish to thank the R community and open source software developers in general. Open source tools make science more accessible and the readiness of the community to help each other out to learn these tools is overwhelming. It is inspiring to see science advance as a result of human curiosity and collegiality instead of profit incentives.

Abstract

Crown shyness describes the phenomenon in which tree crowns avoid growing into each other, producing an impressive puzzle-like pattern of complementary tree crowns in the canopy. Previous studies defined crown shyness in terms of canopy cover or intercrown distance and found that crown shyness is related to structural characteristics of the trees such as tree slenderness and size differences. This study aimed to expand the current set of models for crown shyness by quantifying the characteristic of surface complementarity among tree crowns displaying crown shyness using terrestrial LiDAR data. Subsequently, the relationship between crown surface complementarity and structural characteristics of the trees was analysed to verify whether previous models for crown shyness show agreement with the model developed in this study.

A metric that quantifies the surface complementarity (S_c) of a pair of docking protein molecules is adopted from Lawrence and Colman (1993) and applied to the point clouds of pairs of adjacent trees. Three-dimensional tree crown surfaces were generated from the point clouds by computing their α-shapes. Pairs that were visually determined to be overlapping scored significantly lower S_c values than pairs that did not overlap (n=14, $p < 0.01$). Furthermore, average slenderness of a pair of trees correlated positively with their S_c-score ($R^2 = 0.49$, $p < 0.01$), showing accordance with previous studies on crown shyness.

The results indicate that the 3D model for crown shyness developed in this study may contribute to future research on crown shyness. However, testing the model on a larger set of pairs is necessary to confirm its usefulness.

Keywords: crown shyness, complementarity, alphashapes, terrestrial LiDAR, forest canopy, tree slenderness

Contents

1 Introduction

1.1 Context & background

Forest structure can be defined as the spatial arrangement of above-ground biomass in a forest (Von Gadow and Hui, 2002). Examples of forest structural characteristics include the proportions of different size classes, the number of layers in the canopy, and the spacing between trees (Figure 1, (Aguirre et al., 2003; West et al., 2009; Bohlman and Pacala, 2012)). Forest structure plays a key role in many ecological processes and determines to a large degree the functioning of a forest ecosystem. For example, previous studies have shown that forest structure influences primary productivity as it determines the way forests capture sunlight (Ishii et al., 2004; Hardiman et al., 2011, 2013; Williams et al., 2017). Moreover, forest structure affects animal and plant communities by the way it shapes habitats in the forest. (Tews et al., 2004; Burrascano et al., 2008; Halpern and Spies, 2008). Additionally, forest structure may regulate a forest's resilience against disturbances such as windthrow (Ryan, 2002) and fire (Everham and Brokaw, 1996).

Figure 1: Schematic drawing of a forest's structure.[1] Some structural characteristics visible in the drawing are the presence of a multi-layered canopy, a diverse range of tree sizes and closely spaced trees.

Interactions between tree crowns influence forest structure by changing the way trees grow (Muth and Bazzaz, 2003). The vertical and horizontal distributions of branch and foliage material are the result of competition for canopy space between adjacent trees (Getzin et al., 2006; Rouvinen and Kuuluvainen, 2011). Competition can lead trees to grow asymmetrical crowns instead of their 'ideal' symmetrical shape. The ability of trees to adapt the shape of their crown in response to the presence of adjacent trees is called 'crown shyness' (Jucker et al. (2015), Figure 2). Trees that experience intense competition due to high tree densities show stronger crown plasticity, attempting to grow in the direction of unoccupied spaces in the canopy (Schröter et al., 2012; Jucker et al., 2015).

[1]Food and Agriculture Organisation, retrieved from http://www.fao.org/3/T0178E/T0178E02.gif on 26/09/2019

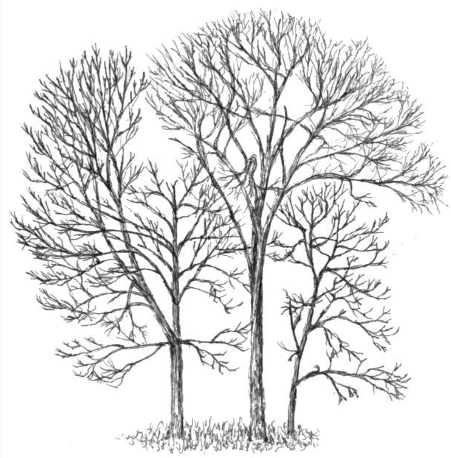

Figure 2: A group of trees growing asymmetrical crowns as a result of crown plasticity. [2]

Tree crowns sometimes show a degree of ‘crown shyness’ where tree crowns avoid full canopy closure by leaving small channel-like gaps between their crowns (Figure 3). Crown shyness has been attributed to avoidance of mutual shading (Ballare et al., 1997; Franklin and Whitelam, 2005) and mechanical abrasion of the outer twigs (Putz et al., 1984; Meng et al., 2006). These two processes may induce morphological changes in individual tree crowns that result in crown shyness.

To avoid mutual shading, trees sense nearby trees with ‘phytochromes’. Phytochromes are pigments that are sensitive to red (655-665 nm) and far-red light (725-735 nm) (Li et al., 2011). As light interacts with plant material, the red/far-red ratio decreases (Aphalo et al., 1999). When light with a decreased red /far-red ratio is recorded in the phytochromes, a tree may direct growth away from the source of this light (Gilbert et al., 1995). The adaptation of growth direction may result in the formation of gaps between the trees. Crown plasticity is stronger among adjacent trees of unequal sizes, likely because suppressed trees invest more in avoiding their large neighbours (Muth and Bazzaz, 2003). This may result in stronger crown shyness between trees that are of unequal size.

Alternatively, in the abrasion theory wind plays an important role (Putz et al., 1984). Rudnicki et al. (2001) conducted an experiment in which trees were tied to each other making them sway simultaneously under windy conditions. This prevented their branches from colliding and as a result the space between crowns drastically declined. Moreover, another study showed that trees inhibit twig regrowth after taking damage from abrasion, creating space between neighbouring crowns (Hossain and Caspersen, 2012). Tree slenderness, the ratio between tree height and stem diameter, is associated with more frequent and intense collisions between trees (Rudnicki et al., 2003; Fish et al., 2006). Furthermore, branches of trees with low wood density are more likely to break in a collision (Van Gelder et al., 2006). It is expected crown shyness is stronger among slender trees and trees with low wood density.

The ability of trees to sense neighbouring trees and adapt their crown shape accordingly is an important factor in the constitution of forest canopy structure. The process of trees optimizing canopy space capture while avoiding neighbouring tree crowns results in the formation of complementary crown shapes. This is also visible in Figure 3, where the surfaces of the tree crowns seem to fit into each other like puzzle pieces.

[2] Craig Holdrege, retrieved from http://natureinstitute.org/pub/ic/ic14/trees.pdf on 26/09/2019

Figure 3: Camphor trees displaying crown shyness. [3]

The ability of trees to sense neighbouring trees and adapt their crown shape accordingly is an important factor in the constitution of forest canopy structure. The process of trees optimizing canopy space capture while avoiding neighbouring tree crowns results in the formation of complementary crown shapes. This is also visible in Figure 3, where the surfaces of the tree crowns seem to fit into each other like puzzle pieces, complementing each other's shapes.

'Complementarity' is a frequently used concept in ecological science and is often described as an important biological mechanism through which species and functional diversity affect ecosystem functioning (Morin et al., 2011; Tilman and Snell-Rood, 2014). Complementarity can be broadly defined as differences between organisms which allow coexistence of the organisms (Petchey, 2003). Complementarity may manifest itself in many different forms: differences in animal diets (trophic complementarity, Poisot et al. (2013); Peralta et al. (2014)), pollinators visiting flowers at different moments (temporal complementarity, Venjakob et al. (2016)) or differences in rooting strategies and tree crown architecture (spatial complementarity, Ishii and Asano (2010); Liu et al. (2015)).

1.2 Problem statement

Forest canopy structure is difficult to measure (Watt and Donoghue, 2005). Research on forest canopies and tree crowns has been impeded by laborious and suboptimal measuring techniques. Examples of traditional techniques include sampling of crowns into a limited number of radii (Krajicek et al., 1961; Fish et al., 2006; Goudie et al., 2009) or visual estimation of intercrown spacing (Putz et al., 1984). Apart from being time consuming and error prone, these techniques also fail to represent the full three-dimensional structure of trees. So far, much research on aboveground interaction between trees has relied on two-dimensional polygon projections of tree crowns (Lorimer, 1983; Rudnicki et al., 2001; Goudie et al., 2009; Pretzsch et al., 2015), see Figure 4. These projections are a simplification of the detailed structure of a tree crown and taking such an approach comes with an inevitable loss of information (Vierling et al., 2008).

[3] Patrice78500, retrieved from https://commons.wikimedia.org/wiki/File:Dryobalanops_Aromatica_canopy.jpg on 26/09/2019

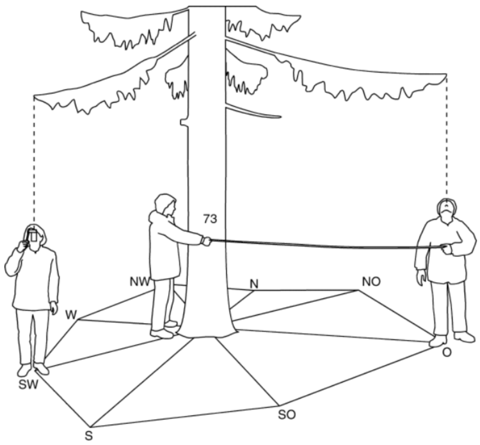

Figure 4: Manual crown projection measurement[4]

The lack of detailed data on tree crown geometry has limited research on spatial complementarity of tree crowns. Recent studies have quantified complementarity of crown volumes for a pair of trees by calculating the difference of crown volumes over a range of vertical strata (Williams et al., 2017; Zheng et al., 2019). Based on the reviewed literature no research has been conducted on the complementarity of tree crown surfaces. Surface complementarity modeling is popular in molecular biology where the complementarity of protein molecule surfaces plays an important role in protein aggregation (Li et al., 2013). Many molecule surface complementarity estimators quantify complementarity by assessing the degree to which concave and convex sections of a pair of molecule surfaces coincide (Figure 5, Lawrence and Colman (1993); Norel et al. (1994)). This method can prove useful for quantifying crown surface complementarity provided there is suitable data for a similar computation.

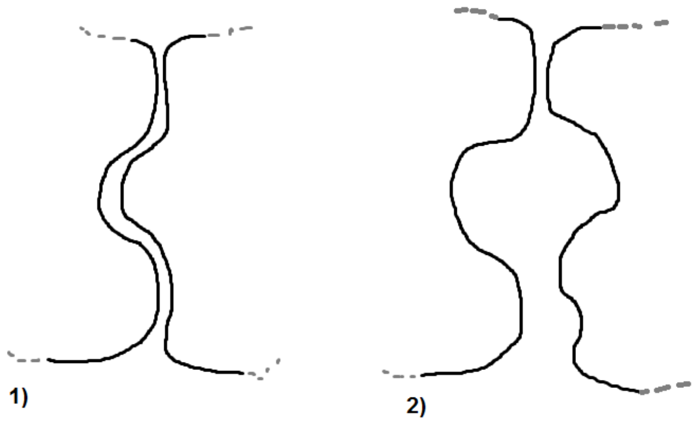

Figure 5: 2D schematic drawing of two protein molecule surfaces interacting. In situation 1) the molecules are complementary: convex sections in the surface of one molecule coincide with concave sections in the surface of the other, maximizing surface contact. In situation 2) the opposite is the case: concave sections of both molecule surfaces coincide leaving a gap of empty space resulting in less surface contact.

[4]Illustration from Pretzsch et al. (2015)

LiDAR (Light Detection and Ranging) has the ability to capture the three-dimensional structure of trees. A scanning device sends out a large amount of laser pulses of which it records direction and travel time when scattered back by a hard surface. With this information it is possible to construct a 3D point cloud in which the points represent every location where a laser pulse was backscattered (Lim, 2006).

Terrestrial LiDAR systems scan inside the forest, close to the targets (Dassot et al., 2011). The introduction of terrestrial LiDAR in forest settings is revolutionizing research on the structure of trees and forests (Malhi et al., 2018). The availability of highly detailed tree structure data is driving advances in traditional forest ecological challenges. Examples of this include improved models of above-ground tree biomass (Calders et al., 2015; Gonzalez de Tanago et al., 2018), leaf area distribution (Tang et al., 2014), and three-dimensional tree archtitecture (Lau et al., 2018; Malhi et al., 2018). Terrestrial LiDAR is a promising technique for advancing forest ecology, but in order to use its full potential, methods have to be developed to extract the bountiful information from point cloud data.

Point clouds derived from LiDAR can be analyzed using computer algorithms. These algorithms often involve a set of chosen parameters that determine the outcome of the analysis. For example, studies on tree volume estimation using voxelized point clouds showed that choice of voxel size may strongly influence the volume measurements (Béland et al., 2014; Lecigne et al., 2018). While volume estimates from point clouds can still be feasibly validated with ground measurements (Calders et al., 2015; Gonzalez de Tanago et al., 2018) more complex metrics may be computed for which no validation data exists (Palace et al., 2016; Atkins et al., 2018). A sensitivity analysis on the algorithm parameters can then still provide an understanding of the uncertainty in the measurements of such metrics (Trucano et al., 2006).

1.3 Research Objectives and Research Questions

This study aims to find methods for quantifying spatial complementarity of tree crown surfaces using point cloud data. Sensitivity of the analysis to parameter choice is considered to explore how robust the methods are. Finally, the role of size and architectural differences between neighbouring trees in the constitution of complementary crown shapes is analyzed.

To fulfill the aim of this research the following research questions will be addressed:

- RQ1: How can spatial complementarity of a pair of tree crown surfaces be quantified from individual tree point clouds?
- RQ2: How do analytical parameters affect this measurement?
- RQ3: How does spatial complementarity of a pair of tree crown surfaces vary with different size and structural characteristics of the trees?

2 Methods

2.1 Study site

Terrestrial LiDAR sampling of trees was carried out in January and February 2017 during a field campaign in Guyana for a case study on improving allometric equations for biomass estimation (Lau et al., 2019). The study site was a newly granted logging concession located in the East Berbice region of Guyana (4.48 to 4.56 lat and -58.22 to -58.15 long). The area is covered by dense wet forest and had seen little anthropogenic influence prior to the arrival of the logging company.

2.2 Data

2.2.1 LiDAR data

Over the course of four weeks a total of 106 trees were scanned with a Riegl VZ-400 scanning device using an angular resolution of 0.04°. The trees were scanned from multiple positions in a double circular pattern consisting of an inner ring at 6-8 meters and an outer ring at 11-14 meters from the focal tree (Figure 6). In total 14 pairs among 14 individuals were positioned close enough to be considered a pair with interaction between their crowns. This was based on a visual inspection of the proximity of the two tree crowns. The individual point clouds of those trees were semi-automatically extracted for analysis.

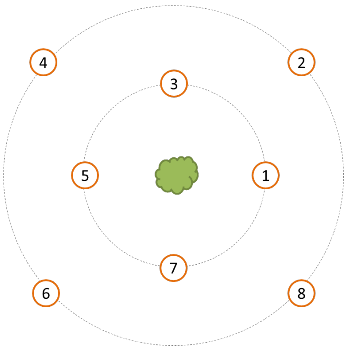

Figure 6: Basic setup of the scanning positions around the tree. Reflective targets were used as tie points to co-register the different scans.

2.2.2 Tree data

The relationship between crown surface complementarity and several variables concerning size and structural properties of the trees will be tested. Size variables include diameter at breast height (DBH) and the height of the trees. The structural properties to be assessed are tree slenderness coefficient (height to DBH ratio) and wood density. Tree height and DBH were measured in situ. Wood density values for the selected tree species are taken from the Global Wood Density Database (Chave et al., 2009).

2.3 Measuring surface complementarity

2.3.1 Theoretical background

A method for quantifying the complementarity of molecule surfaces is adopted and applied to the point clouds of pairs of trees. The method is taken from Lawrence and Colman (1993) who computed pair-wise shape complementarity (from here on also referred to as S_c) of protein molecules.

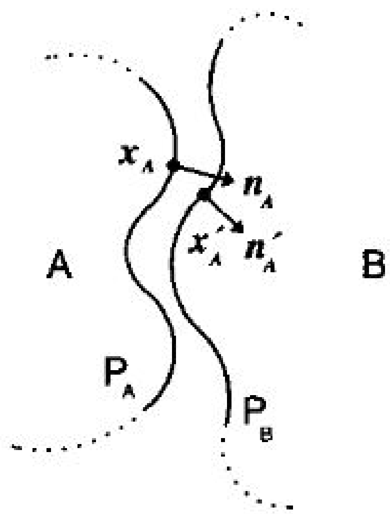

Figure 7: Explanatory schematic drawing of the pairwise complementarity computation, taken from Lawrence and Colman (1993).

Figure 7 shows the idea behind the computation of S_c. A and B are two interacting protein molecules. P_A and P_B (bold continuous lines) are the adjacent parts of the surfaces of A and B. x_A is a point on P_A with n_A as its unit normal vector in the direction of P_B. x'_A is the point on P_B closest to x_A with n'_A as its inward directed unit normal vector. For every point x_A on P_A the dot product of n_A and n'_A can be evaluated:

$$S^{A \to B} = n_{\mathrm{A}} \cdot n'_{\mathrm{A}} \tag{1}$$

The same can be done in the opposite direction for every point x_B on P_B:

$$S^{B \to A} = n_{\mathrm{B}} \cdot n'_{\mathrm{B}} \tag{2}$$

Values of $S^{A \to B}$ and $S^{B \to A}$ can be sampled by evaluating the functions at k points on each of the surfaces P_A and P_B. S_c is then defined as the average of the arithmetic means of the sampled $S^{B \to A}$ and $S^{A \to B}$ values:

$$S_c = \frac{\frac{1}{k}\sum_{i=1}^{k} S_i^{A \to B} + \frac{1}{k}\sum_{i=1}^{k} S_i^{B \to A}}{2} \tag{3}$$

In short, S_c is an average of unit normal vector dot products (Equation 3). The dot product of two unit normal vectors can be interpreted as an expression of how similar the direction of the unit normal vectors are. The value of a unit normal vector dot product ranges from -1 (completely opposed direction of the vectors) to 1 (vector directions perfectly line up). As shown in Figure 8, the value of dot products between the unit normal vectors of two nearest neighbours on a pair of surfaces is related to how convex and concave sections of the surfaces are arranged. The dot product returns negative values when the surfaces overlap (Figure 8A). When convex sections on one surface coincide with convex sections on the other surface, the values of the unit normal vector dot product ranges from 0 to 1 (Figure 8B). The same holds for coincidence of concave sections on both surfaces (Figure 8C). The dot product values equal 1 when convex sections on one surface perfectly coincide with concave sections on the other (Figure 8D).

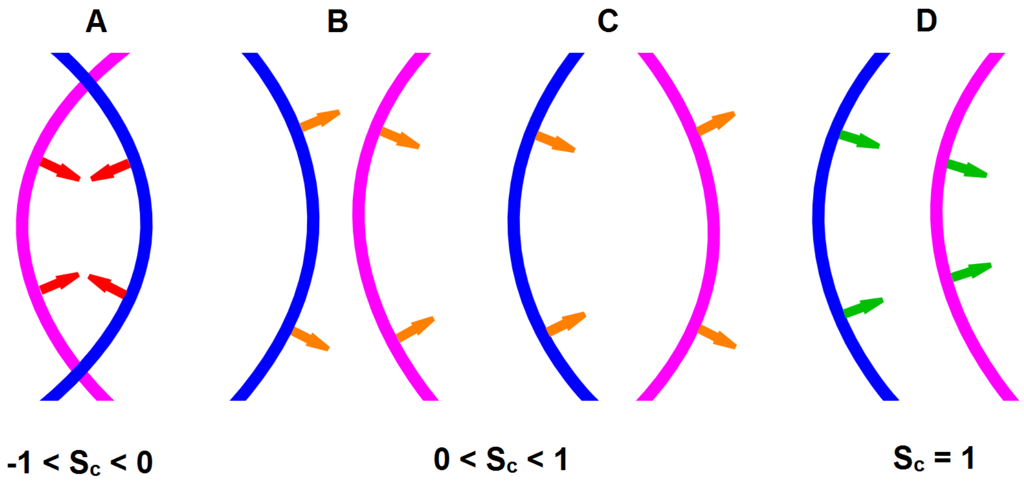

Figure 8: Different arrangements of convex and concave sections with their corresponding S_c values. Situation A depicts two overlapping surface sections. In situation B and C, both surface sections are convex or concave respectively. In situation D a concave section perfectly coincides with a concave section.

By applying this analysis to tree crown surfaces a numerical value for tree crown surface complementarity can be produced. A pair of trees with overlapping tree crown surfaces will score low as a result of the negative values on the overlapping parts. A pair with non-overlapping tree crowns (i.e. a pair that shows crown shyness) scores higher, especially so when concave and convex sections coincide.

2.3.2 Segmentation of the interaction zone

The functions $S^{A\rightarrow B}$ (Equation 1) and $S^{B\rightarrow A}$ (Equation 2) are evaluated at points on those parts of the surfaces that are interacting (P_A and P_B in Figure 7). To improve reproducibility and allow the computation of complementarity values for large amounts of pairs a procedure for the automatic segmentation of the surfaces into interacting and non-interacting parts was developed.

The first step in the procedure is the separation between the bole and the crown of the trees. At this moment the point clouds are voxelized. The voxel points are used to make a vertical profile of the tree point clouds (Figure 9). The number of points strongly increases in the vertical direction from the first branching point onward. The first histogram bin in the vertical direction with a density value larger than a certain threshold marks the bottom of the tree crown. All points with a height value larger than or equal to the height value associated with that bin are selected and classified as tree crown. A density threshold of $p = 0.015$ produced satisfying results for all pairs in this dataset.

The next step is to find the points on a pair of crown surfaces which are close to each other. This was done by performing a two way nearest neighbour search on the points in the crowns (Figure 10). Consider a pair of tree crowns A and B. First, all points in crown A are queried for their nearest neighbour point in crown B. This returns a set of points which are on the surface of crown B and adjacent to crown A. This is also done in the opposite direction, querying points in crown B for their nearest neighbour point in crown A. The resulting two sets of adjacent points are the the input for the next operation.

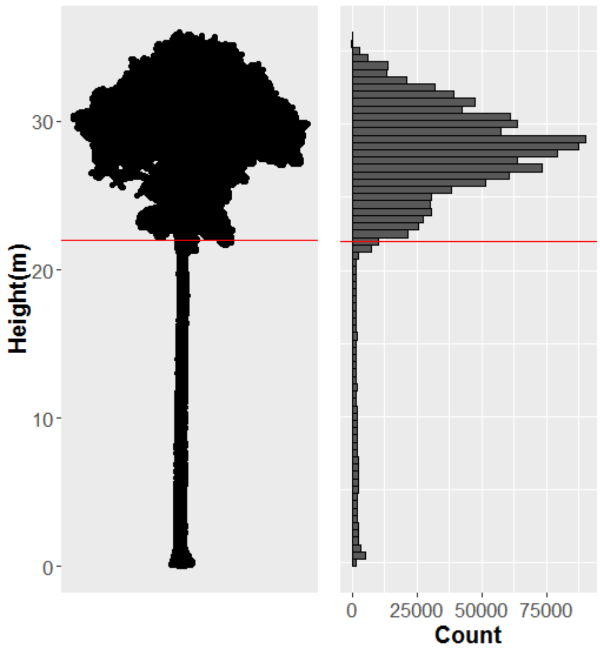

Figure 9: A height projection of a voxelized tree point cloud (left) and its point count histogram of height values (right). The red line indicates the height value associated with the first bin to exceed the threshold density value (set to $p = 0.015$). This threshold is used to delimit the crown area.

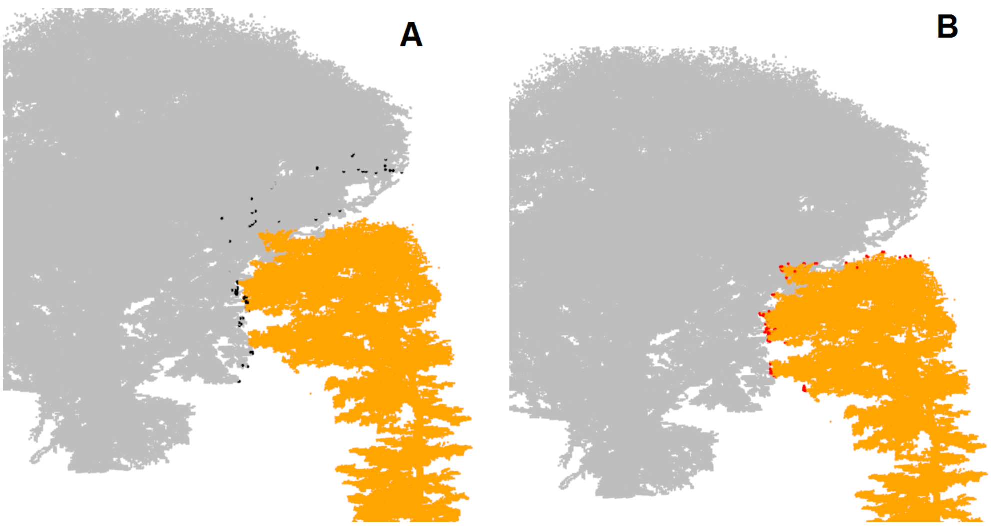

Figure 10: Image A: nearest neighbours (black dots) of all points in the orange tree. Image B: nearest neighbours (red dots) of all points in the grey tree.

Bounding boxes (Figure 11) are created around the union of the two sets of neighbouring points shown in Figure 10. These bounding boxes are used to make a final selection of points that will be the input for the surface generation. The bounding boxes are created by enclosing a volume between six planes. These planes are based on the spread of the neighbouring points.

First two 'axes of interaction' are defined to position the first four planes. The first axis of interaction (green line, Figure 11) is defined as the straight line that connects the centroids of the tree crowns in the XY-plane (purple dots). The set of neighbouring points (red and black, Figure 10) resulting from the two way nearest neighbour search are plotted in the XY-plane above the trees for visibility. Red points belong to the orange tree and are the nearest neighbours to all points in the grey tree. Black points belong to the grey tree and are the nearest neighbours to all points in the orange tree. To determine how far the neighbouring points are spread out in the direction of the first axis of interaction, the set of neighbouring points is projected onto this axis. The projections with the minimum and maximum value of the line equation mark the extent over which the tree crowns interact in this direction. The points corresponding to these projections are marked yellow. Planes are fitted going through these points with the direction vector of the line equation as the normal vectors of the planes.

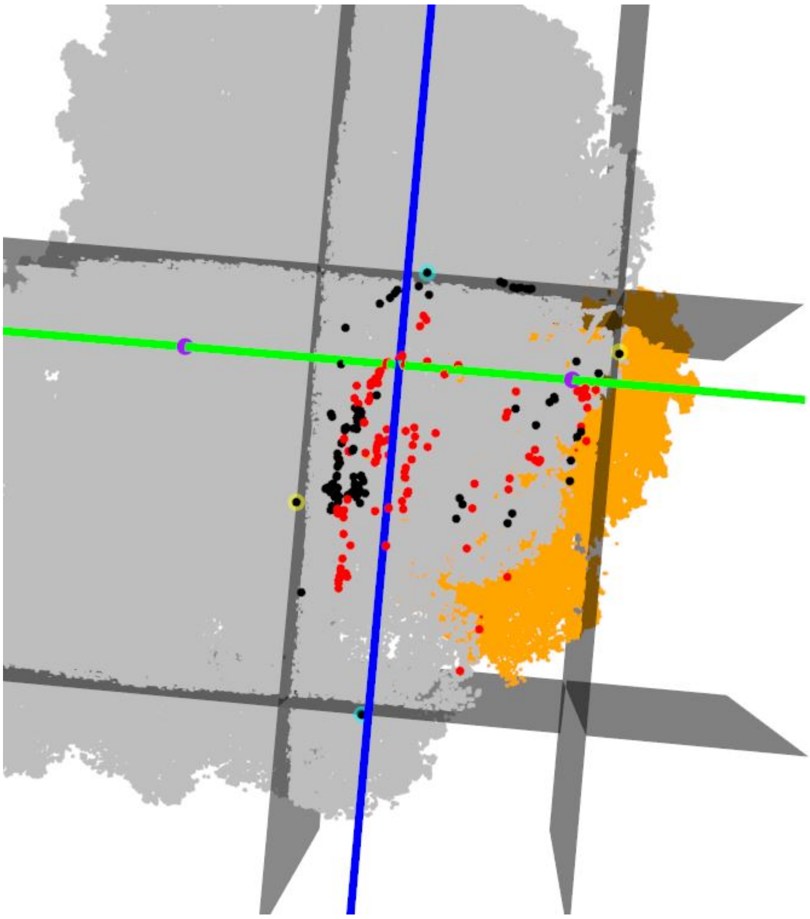

Figure 11: The bounding box as viewed from the top. Black and red points indicate the neighbouring points resulting from the two-way nearest neighbour search (Figure 10A and B respectively), plotted above the trees for visibility. Purple dots are the centroids of the tree crowns, defining the first axis of interaction (green line). The second axis (blue line) is a line perpendicular to the first axis.

The same is done for a second axis of interaction (blue line, Figure 11). This second axis of interaction is defined as the straight line perpendicular to the first line of interaction at an arbitrary point on the first axis of interaction. The neighbouring points are again projected on the perpendicular line. Again planes are fitted at the points with the minimum and maximum value of the perpendicular line equation (coloured light blue), using the direction vector of the perpendicular line equation as the normal vectors of the planes.

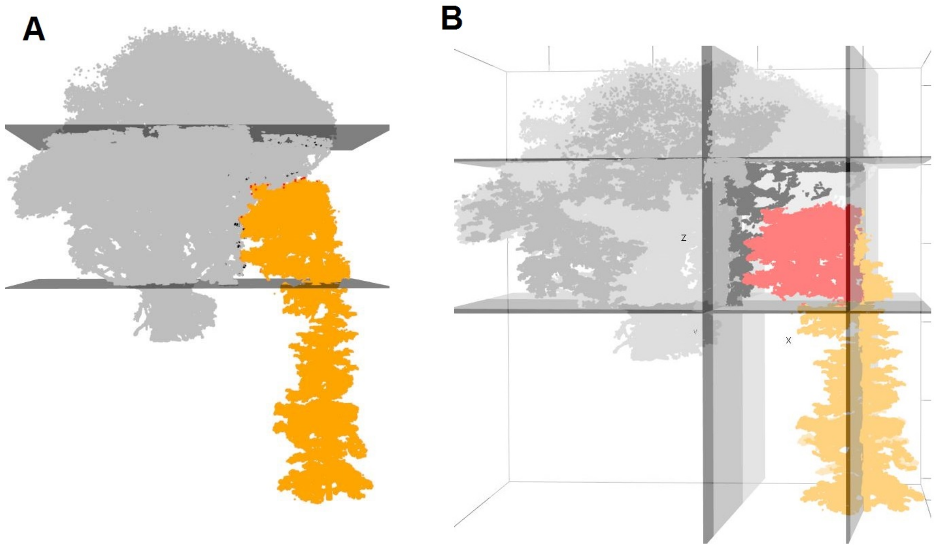

Figure 12: Vertical boundaries of the bounding box (A) and the complete box including the selected points of both trees in black and red (B).

Finally, the upper and lower bounds of the bounding box are defined by horizontal planes at the minimum and maximum height values of the set of neighbouring points (Figure 12A). The six planes together form a bounding box around the set of neighbouring points which contains the interacting parts of the pair of tree crowns (Figure 12B).

2.3.3 Surface generation using α-shapes

A surface is generated for each tree around the sets of points contained in the bounding box by computing the α-shapes of the sets (Edelsbrunner and Mucke, 1994). The α-shape of a point set is a general case of the convex hull. The α parameter determines how convex the shape is. When $\alpha = \infty$ the α-shape of a point set is identical to the convex hull of that point set. Lower α-values allow cavities to be present in the shape. The minimum size of those cavities is proportional to the magnitude of α. This property allows the characterization of both convex and concave sections on the surfaces of the tree crowns.

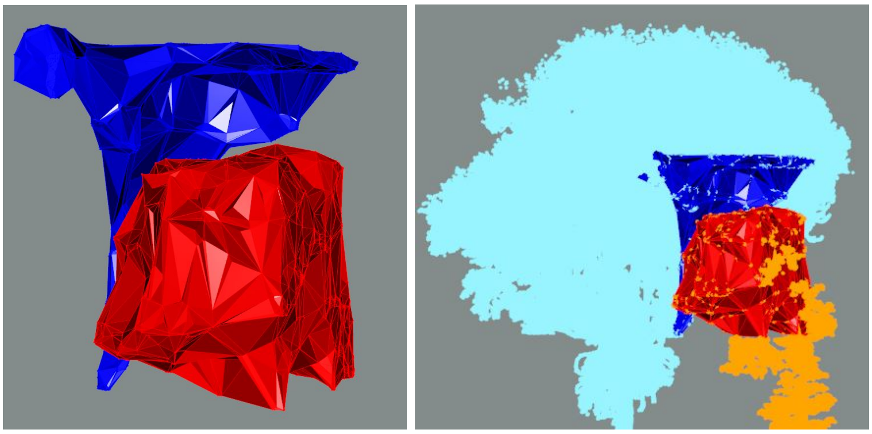

Figure 13: An example of the α-shapes of the interacting parts of a pair of trees.

The α-shape computation is performed in R using the 'alphashape3d' package produced by Lafarge et al. (2014). The computation returns a Delaunay-triangulation of the boundary points of the tree crown as defined by the α-shape. This creates a surface of triangles with normal vectors. The normal vectors of these triangles provide the data needed for the computation of S_c as described in Figure 7.

2.3.4 Sampling the vectors

Not all triangles on the α-shape surfaces are relevant for the computation of S_c. The parts of the α-shapes that are facing away from each other will have had little influence from interactions between the tree crowns. The relevant triangles of the α-shape are selected by performing a two-way nearest neighbour search on the triangle center points (similar to an earlier step in section 2.3.2, see page 10). The normal vectors of the selected triangles are then used in the computation of the S_c value for the pair of tree crown surfaces (Figure 14).

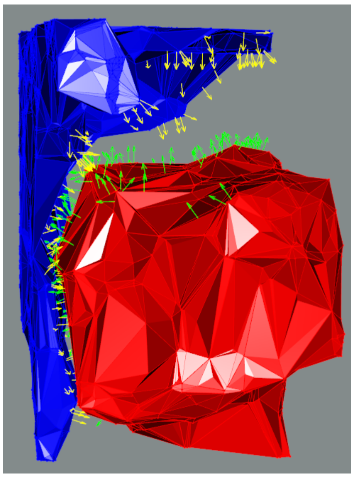

Figure 14: Unit normal vectors of the sampled triangles on the α-shapes.

2.4 Statistics

Differences in surface complementarity between overlapping and non-overlapping pairs of trees were tested using an independent samples t-test. Relationships between crown surface complementarity and tree height, diameter size, slenderness and wood density are tested using simple linear regression. All variables were tested for normality using the Shapiro-Wilk test.

3 Results

3.1 Pair-wise complementarity computations

Complementarity values were succesfully computed for all 14 pairs. Half of the pairs showed a degree of crown overlap. An example is shown in Figure 15, $S_c = 0.16$. The other half had no overlap between their crowns (Figure 14, $S_c = 0.71$).

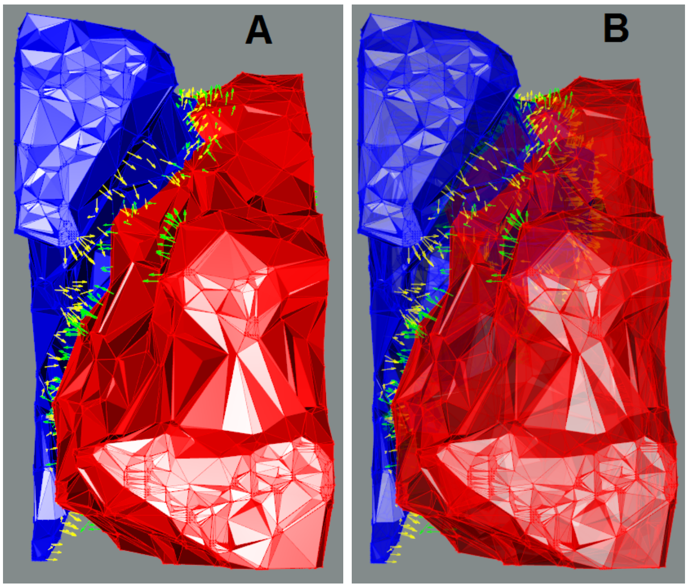

Figure 15: Opaque (A) and transparent (B) α-shapes for a pair of overlapping crowns ($S_c = 0.16$). The transparent α-shapes in image B show the intrusion of a part of the blue crown into the red crown. Voxel size used is 5 cm and $\alpha = 1$.

The complementarity values of the overlapping pairs were significantly lower than those of non-overlapping pairs (Figure 16, significance level 0.05, p = 0.001). The mean S_c value was 0.41 for overlapping crowns and 0.73 for non-overlapping crowns. Both groups contained one outlier. The outlier in the group of overlapping pairs was a pair that had only small sections of overlap compared to other overlapping pairs. The point clouds of the outlier pair in the non-overlapping group were of inferior quality. Point density was much lower compared to other pairs and especially at the edges points were sparsely distributed which may have lead to an incorrect representation of the tree crown surfaces.

3.2 Effect of parameter choice on complementarity measurements

The average S_c value of the 14 pairs fluctuated slightly before the 5 cm voxel size mark (Figure 17). Using voxel sizes larger than 5 cm resulted in lower average S_c values than the smaller voxel sizes (see left panel of Figure 19 for an example using 75 cm voxels). At voxel sizes larger than 75 cm the computation of S_c became impossible for some of the pairs. This was due to the crowns having too little points to perform the α-shape computation.

Sample mean S_c values were relatively low at small α values and increased with larger α values, stabilizing at $\alpha = 1$ (Figure 17). The larger lower quantile and whisker of the boxplot at the lowest α value ($\alpha = 0.2$, see right panel of Figure 19) suggest this effect is more pronounced in pairs with low complementary values. After $\alpha = 2.5$ the mean S_c values of the sample decrease again (Figure 18). The sample median was much less affected by this than the sample mean (Table 1).

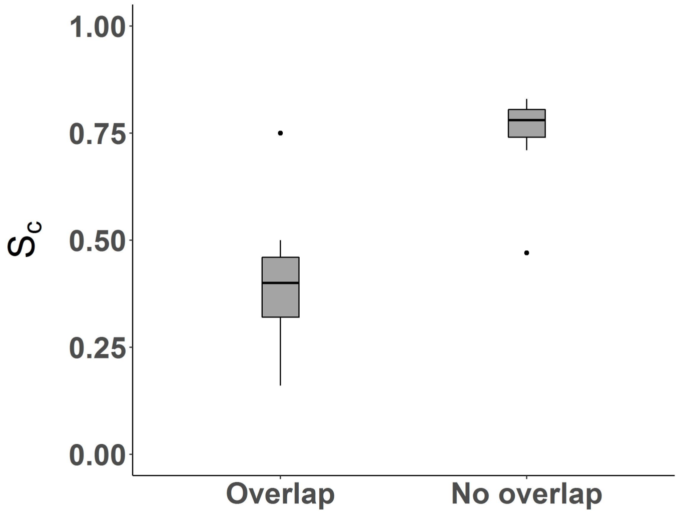

Figure 16: Boxplot of the complementarity values of overlapping and non-overlapping pairs of tree crowns. Black dots represent outliers. Whiskers indicate minimum and maximum values (excluding outliers). Values computed using a voxel size of 5 cm and $\alpha = 1$. Mean S_c of overlapping pairs was significantly lower than non-overlapping pairs (significance level 0.05, p = 0.001).

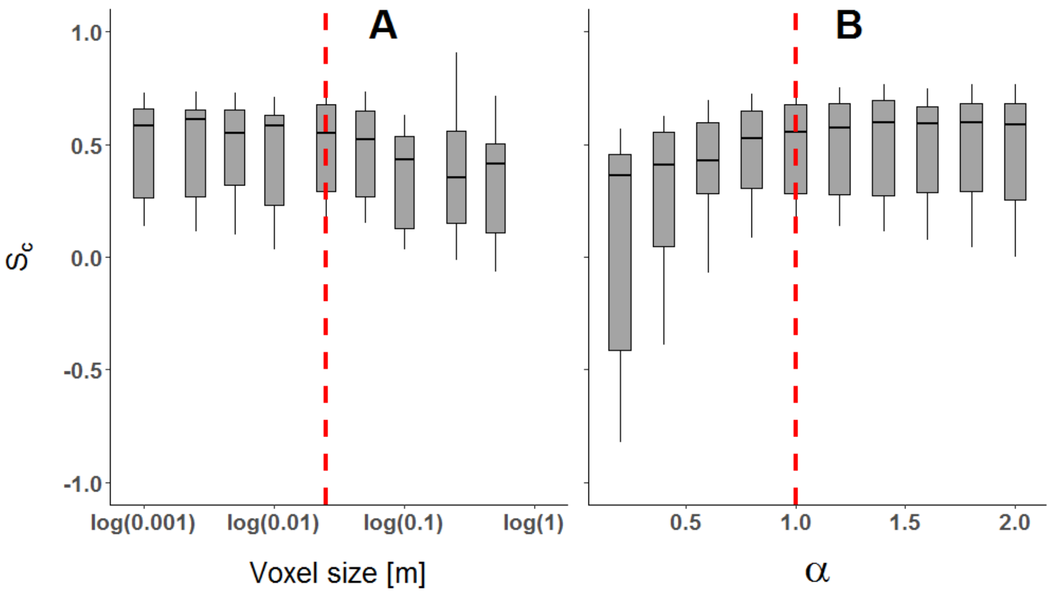

Figure 17: Boxplots of the average S_c value for the whole sample at different settings of voxel size (graph A) and α (graph B). Red dashed lines indicate where the average S_c value stabilizes (voxel size 0.05m and $\alpha = 1$). Voxel sizes are on a log scale.

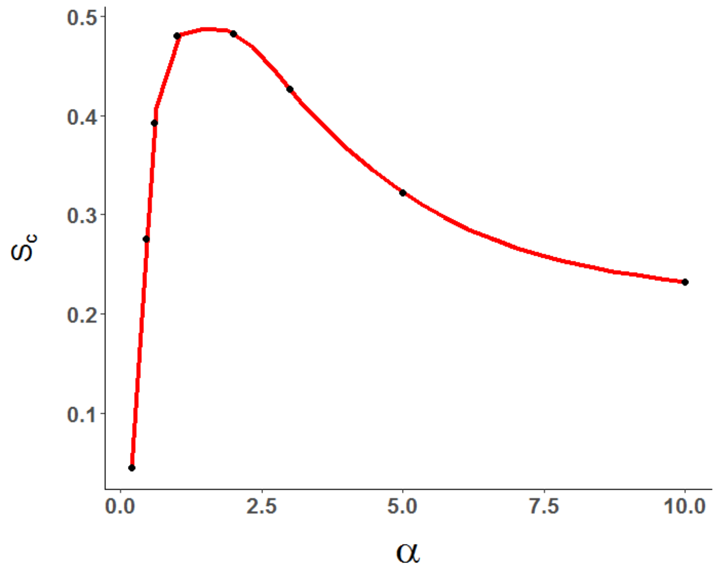

Figure 18: Average sample S_c for a range of α-values (black dots). Red line is a smooth interpolation of the data points. Values computed using 5 cm voxel size.

Table 1: Sample mean and median surface complementarity values using a range of α values. Values computed using 5 cm voxel size.

α	**Mean** S_c	**Median** S_c
0.2	0.05	0.36
0.4	0.28	0.41
0.6	0.39	0.43
1	0.48	0.55
2	0.48	0.59
3	0.43	0.56
5	0.32	0.43
10	0.23	0.29

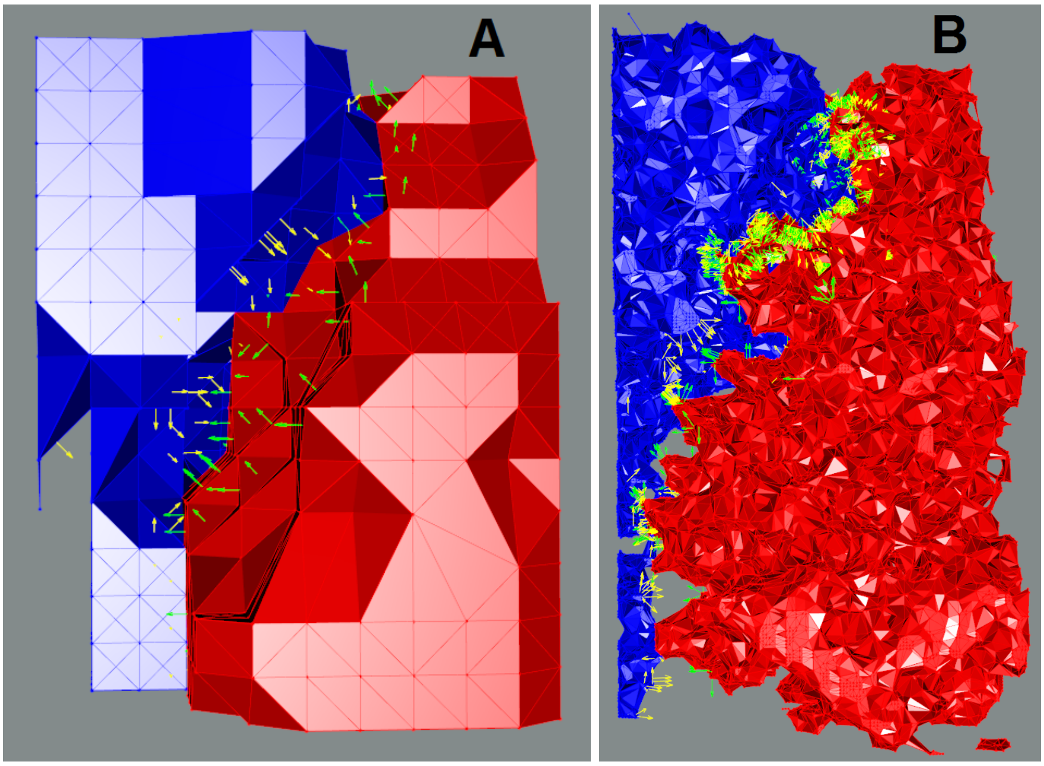

Figure 19: α-shapes of the same pair of trees as in Figure 15. The α-shape in image A is computed using a voxel size of 75 cm and $\alpha = 1$. The α-shape in image B is computed using a voxel size of 5 cm and $\alpha = 0.2$.

3.3 Tree size asymmetry, structure and surface complementarity

Tree size asymmetry was expressed using a ratio index of the trees in a pair. A size ratio of 1 indicates the trees in the pair have the same size. Lower values mean the trees are less equal in size. Pairs consisting of trees of less equal size scored higher S_c values (Figure 20). The tree structure of a pair was characterized by computing the average wood density and the average slenderness coefficient of the pair. Low wood density and high slenderness coefficient were associated with high crown surface complementarity values (Figure 21).

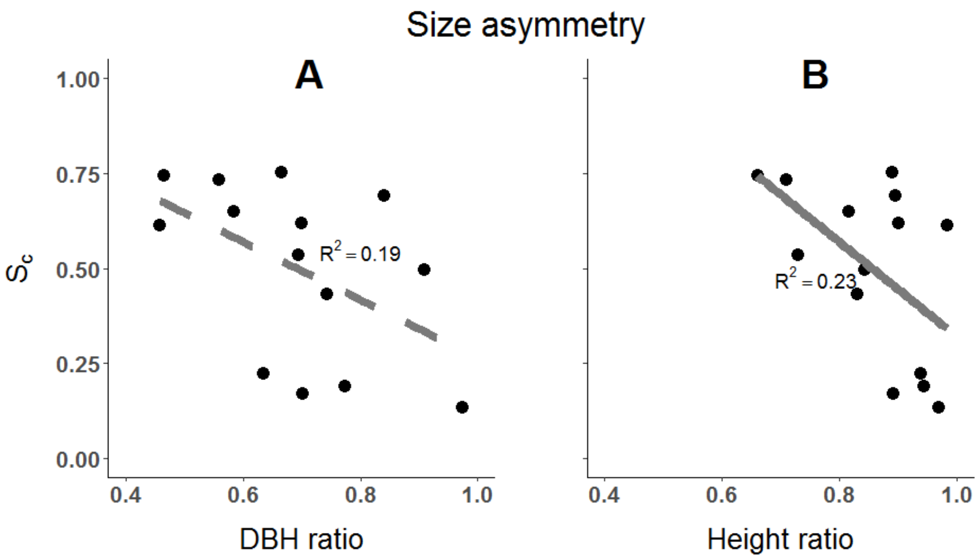

Figure 20: Simple linear regressions of crown surface complementarity and size ratios. Both DBH (graph A) and height ratio (graph B) showed a negative association with crown surface complementarity. This relationship was significant for tree height ratio (solid line, p=0.048 and $R^2 = 0.23$) but not for DBH ratio (dashed line, p=0.067 and $R^2 = 0.19$) at the 0.05 significance level. S_c values were calculated using $\alpha = 1$ and a voxel size of 5 cm.

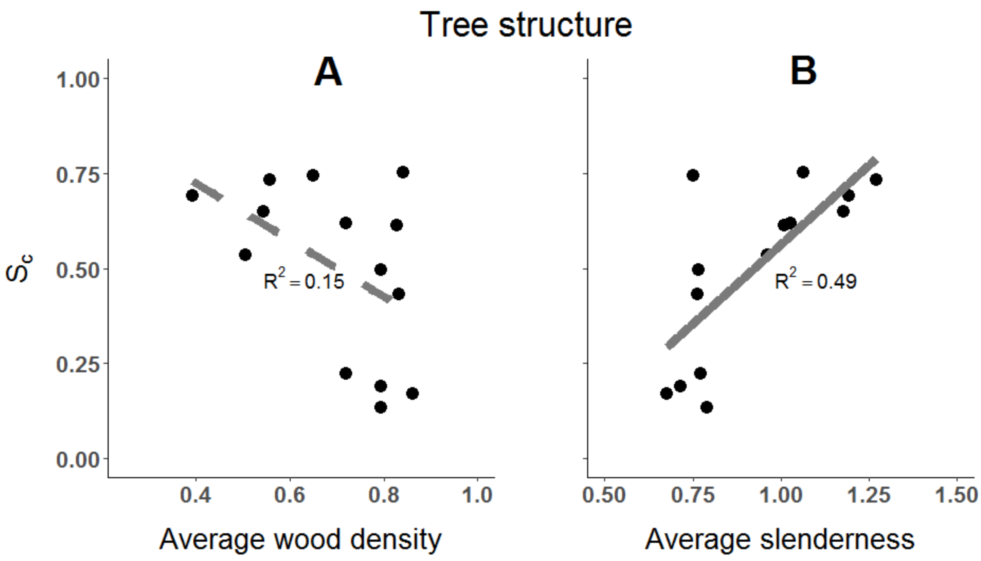

Figure 21: Simple linear regressions of crown surface complementarity and tree structure characteristics. Wood density was negatively associated with crown surface complimentarity (graph A), while slenderness showed a strong positive correlation (graph B). The relation was significant for slenderness (solid line, p=0.003 and $R^2 = 0.49$) but not for Average wood density (dashed line, p=0.067 and $R^2 = 0.15$) at the 0.05 significance level. S_c values were calculated using $\alpha = 1$ and a voxel size of 5 cm.

4 Discussion

4.1 Crown overlap and surface complementarity

A metric for surface complementarity, S_c, was adopted from Lawrence and Colman (1993) and applied to point clouds of pairs of trees. This enabled the quantification of the puzzle-like pattern present in groups of tree crowns exhibiting crown shyness. The method produced sensible results as overlapping crowns scored significantly lower in surface complementarity compared to non-overlapping crowns (Figure 16). The surface complementarity values of non-overlapping crowns are similar to those that Lawrence and Colman found for the complexes of proteins they analyzed which ranged from 0.64 to 0.74. Since their models for molecules did not allow overlapping they did not find such low values as for the overlapping crowns in this study.

Studies on other types of complementarity also see overlap as a sign of low complementarity (Mason et al., 2008; Blüthgen and Klein, 2011; Aguiar et al., 2013; Poisot et al., 2013). Those studies examined a particular trait related to resource use such as an animal's diets (Poisot et al., 2013; Aguiar et al., 2013) or the shade tolerance of a plant (Chen et al., 2016; Van de Peer et al., 2018). When such traits overlap between organisms they are considered to be competing with each other (Mason et al., 2011). Niche partitioning is the process of organisms minimizing this overlap in order to reduce competition (Silvertown, 2004; Fish et al., 2006). Partitioning not only occurs in terms of dietary or productivity traits but also in spatial dimensions (Lewis and Murray, 1993; Nicholls and Racey, 2006; Albrecht et al., 2009). In this light, crown shyness can be seen as the result of the spatial partitioning of tree crowns in an attempt to avoid direct competition from overlapping while optimizing the use of space available for growth (Franco, 1986). The surface complementarity metric developed in this study can help to determine how effective a pair of trees is at using growing space without overlapping.

4.2 The role of tree structure in crown shyness

For trees to be able to adapt their growth and avoid overlapping they need to be aware of each other's presence. The results of this study support the theory that physical contact plays a role in the formation of crown shyness. The average slenderness of a pair of trees showed a clear positive relationship with the level of shape complementarity between the pair (Figure 21). Trees are sessile organisms but wind can make them sway around, sometimes leading to crown collisions with adjacent trees. Slender trees sway more in the wind and are therefore more likely to collide with one another (Rudnicki et al., 2008). Crown collisions may affect the shape of the crown through reoriented growth after physical touch stimuli (Jaffe et al., 1985; Telewski and Jaffe, 1986; Chehab et al., 2009) or the abrasion of twigs (Putz et al., 1984). Pairs of slender trees may achieve more complementary crown surfaces as the result of a higher frequency of physical contact between their crowns.

Average wood density of a pair of tree was negatively associated with surface complementarity, although not signifcantly (Figure 21). A possible explanation for the negative correlation is the higher probability of branches breaking due to the low wood density. Anten and Schieving (2010) as well as Van Gelder et al. (2006) found a positive relation between wood density and branch stability. Crown collisions may therefore have a larger effect on low wood density trees than high wood density trees. Moreover, low wood density has been related to the shade tolerance of a tree. In general, light-demanding tree species have a low wood density while shade tolerant species have a high wood density (Van Gelder et al., 2006; Poorter et al., 2006, 2012). It is expected that a light-demanding tree invests more in shade avoidance and may therefore divert growth away from adjacent trees at an earlier stage than a shade tolerant tree. Light-demanding plant species in particular have been shown to adapt the direction of their growth as a response to mechanical stimulation as well as changes in light quality and quantity (Pierik and De Wit, 2014).

4.3 The effect of differences in tree height and diameter size

A significant (significance level 0.05, p=0.048) negative relationship between tree height ratio and surface complementarity was observed (Figure 20). A similar relationship was found for DBH ratio, but this relationship was not significant. Height being a more important factor in shading may explain the fact that the relationship is stronger for height ratio than for DBH ratio. This finding is in line with studies on size-asymmetrical competition which found that large height inequality between trees can induce strong morphological changes in the suppressed trees to reduce shading (Grams and Andersen, 2007; Thorpe et al., 2010). These morphological changes may lead to a pair of trees adapting their crown shapes to each other resulting in complementary crown shapes.

4.4 Parameter choice

Choice of voxel size influenced the measurements of the average surface complementarity of the sample (Figure 17). The average surface complementarity values were similar at voxel sizes under 5 cm while computations using voxel sizes larger than 5 cm produced different and lower surface complementarity values. This may be explained by overestimation of the crown dimensions at low voxel resolutions. Vonderach et al. (2012) found that the volume of small branches were subjective to overestimation when large voxel sizes were used. The same may apply to the edges of tree crowns considering they consist of fine material such as twigs and leaves. This can lead to situations where the crowns of two trees do not overlap in reality but their low resolution voxel representations do because of volume overestimation at the edges resulting in lower S_c-values.

The α-value determines the level of detail of the α-shape surface. The smaller the value, the smaller the cavities in the surface are. Higher α-values increase the minimum size of the cavities, leading to a more convex surface (Edelsbrunner and Mucke, 1994). The selected α-value affected the measurement result in several ways. The sample mean surface complementarity value increased considerably over the range from 0 to 1 (Figure 17 and 18). This effect was strong for the sample mean but not for the sample median (Table 1), indicating that pairs scoring high complementarity values were less affected by this than the overlapping pairs scoring low complementarity values. When the α-shape using $\alpha = 0.2$ from Figure 19 is compared with the α-shape using $\alpha = 1$ in Figure 15, it becomes clear that the surface triangles are much smaller when a lower α-value is used. As a result, the nearest neighbour search for sampling the α-shape triangles on the α-shape using a low α-value returns many more points in the top part of the crowns where they are overlapping than on other, non-overlapping parts of the crown surface. This may explain the different responses of overlapping and non-overlapping crowns to α-shape computations using a low α-value.

In the range $1 < \alpha < 2$ the computations produced stable results. In this range the surfaces produced by the α-shape computations are less cluttered and the previously mentioned oversampling in overlapping parts does not occur. The decrease in mean surface complementarity of the sample when using α-values larger than 2 can be attributed to the loss of concave features of the tree crowns as the α-shapes approach the convex hull of the tree point clouds. The increased convexity of the α-shapes leads to lower surface complementarity values through a higher likelihood of overlapping and the conjunction of convex surface parts (Figure 8 A and B).

Using α-shapes computed with $1 < \alpha < 2$ it was possible to capture conjunctions of convex and concave sections of the tree crown surfaces without the overemphasis of overlap present in α-shapes using α-values lower than 1 or the loss of concave features of the tree crowns resulting from higher α-values. Existing literature on the use of α-shapes for 3D tree modelling shows different approaches to choosing the appropriate α-value. Two studies using α-shape metrics as input for a tree species classification model computed α-shapes using several α-values and then chose the value at which the classification model produces the best results (Tokola et al., 2008; Vauhkonen et al., 2009). At low α-values the α-shapes sometimes consist of multiple components rather than a single connected one. Some studies 'optimized' the α-value by selecting the smallest α-value for which the α-shape consisted of a single connected component (Xiao et al., 2012; Korhonen et al., 2013). This implies using a different α-value for every tree rather than a fixed one for the whole sample. Considering the α-value determines the level of detail of the α-shape it makes sense to use a value that fits the objective of the study being conducted. For example, when studying crown surface respiration the surface area of soft materials such as leaves and twigs is important to consider so a high level of detail and therefore a low α-value is advisable, while crown volume estimates can already be accurately achieved using the coarsely detailed convex hull of a tree (Fernández-Sarría et al., 2013).

4.5 Limitations

This study used the 'alphashape3d' package by Lafarge et al. (2014) to generate crown surfaces to be used in the shape complementarity method from Lawrence and Colman (1993). The computation of the final surface complementarity value involves taking the arithmetic mean of sampled the unit normal vector dot products (Figure 7, section 2.3.1). The arithmetic mean is appropriate in the study of Lawrence and Colman (1993) as their surface models consist of uniformly distributed and equally sized triangles. The surface models produced by the alphashape3d package do not have this property and the triangles can differ in size. For example, the α-shape in Figure 15 shows a wide range of triangle sizes. Therefore a weighted mean would be more appropriate to use, whereby the sizes of the triangles used for a particular unit vector dot product should be taken into account. This way small and large triangles contribute to the final surface complementarity value relative to their size. A possible way of weighting would be to sum the surface area of the two triangles involved and weight the computed dot product by the proportion they make up of the combined surface area of the α-shapes. Taking such an approach would give a more accurate description of the surface complementarity of a pair of crowns.

A major limitation of this study was the marginal availability of point clouds of adjacent trees. Out of a total of 106 trees that were scanned during the 2017 campaign in Guyana, only 14 trees were close enough to be considered adjacent. Those trees made up the 14 pairs of trees analyzed in this study which meant that some trees were in more than one pair. The result was a small, geographically limited and not completely independent sample. This makes it difficult to derive meaning from the relationships found in section 3.3. A larger sample size consisting of completely independent pairs would provide a more reliable basis for statistical inference.

Related to this is the issue of scalability. Although the methods used in this study are fully automated, they rely heavily on high quality and correctly segmented point clouds. Small differences in the allocation of points to the trees may lead to large changes in the resulting surface complementarity value. For example, when a branch of a tree is wrongly assigned to another tree it may seem in the point clouds as if the tree crowns overlap while in reality they do not. For a sample of 14 trees it was viable to manually check for such errors but as more point cloud data becomes available this procedure becomes increasingly laborious. Many efforts are being made to improve individual tree segmentation methods (Itakura and Hosoi, 2018; Yan et al., 2018; Williams et al., 2019) however distinguishing tree crowns especially is structurally complex forests remains one of the main challenges (Burt et al., 2019).

5 Conclusions and recommendations

Crown shyness has boggled the minds of forest researchers for decades. This study used terrestrial LiDAR data to shed a new light on crown shyness. The adoption of a method from molecular biology enabled the quantification of the puzzle-like pattern of complementary crown surfaces that is characteristic for groups of trees displaying crown shyness. Crown surface complementarity of pairs of trees exhibited relationships to tree size and structure that were in agreement with existing literature on crown shyness, in particular the importance of tree slenderness in consituting crown shyness.

Terrestrial LiDAR data is radically changing the way we observe forests. Computing plays a crucial role in the retrieval of information from terrestrial LiDAR data. Algorithms designed to measure point clouds often use a set of parameters that determine the outcome of the measurement. This study showed that the choice for a particular parameter setting affects the measuring result. When choosing parameter settings it is important to analyze and understand the effect of your choice on the measurement and to keep in mind what level of detail is appropriate for the research objectives in question.

Further research on this topic should consist of increasing the sample size and including trees from different regions and forest types. Such research may be able to find stronger relationships between crown shyness and tree size and structure and allow a more general interpretation of such relationships. Furthermore the surface complementarity computation could be improved by including a weighted mean instead of an arithmetic mean to increase the accuracy of the measurement.

The metric for crown surface complementarity developed in this study may prove useful in studies on spatial partitioning of the canopy under the influence of environmental factors such as light availability or wind intensity. Understanding how crown collisions and competition for light shape tree crowns may provide valuable insights into why forest are structured the way they are.

6 Bibliography

Aguiar, C. M., G. M. M. Santos, C. F. Martins, and S. J. Presley
2013. Trophic niche breadth and niche overlap in a guild of flower-visiting bees in a Brazilian dry forest. *Apidologie*, 44(2):153–162.

Aguirre, O., G. Hui, K. Von Gadow, and J. Jiménez
2003. An analysis of spatial forest structure using neighbourhood-based variables. *Forest Ecology and Management*, 183(1-3):137–145.

Albrecht, A. M., N. J. Gotelli, and M. Albrecht
2009. International Association for Ecology Spatial and Temporal Niche Partitioning in Grassland Ants. *Oecologia*, 126(1):134–141.

Anten, N. P. R. and F. Schieving
2010. The role of wood mass density and mechanical constraints in the economy of tree architecture. *American Naturalist*, 175(2):250–260.

Aphalo, P. J., A. L. Scopel, and C. L. Ballare
1999. Plant – plant signalling , the shade-avoidance response and competition. *Journal of Experimental Botany*, 50(340):1629–1634.

Atkins, J. W., G. Bohrer, R. T. Fahey, B. S. Hardiman, T. H. Morin, A. E. Stovall, N. Zimmerman, and C. M. Gough
2018. Quantifying vegetation and canopy structural complexity from terrestrial LiDAR data using the forestr r package. *Methods in Ecology and Evolution*, 9(10):2057–2066.

Ballare, C. L., A. L. Scopel, and R. A. Sanchez
1997. Foraging for light: photosensory ecology and agricultural implications. *Plant, Cell and Environment*, 20(6):820–825.

Béland, M., D. D. Baldocchi, J. L. Widlowski, R. A. Fournier, and M. M. Verstraete
2014. On seeing the wood from the leaves and the role of voxel size in determining leaf area distribution of forests with terrestrial LiDAR. *Agricultural and Forest Meteorology*, 184:82–97.

Blüthgen, N. and A. M. Klein
2011. Functional complementarity and specialisation: The role of biodiversity in plant-pollinator interactions. *Basic and Applied Ecology*, 12(4):282–291.

Bohlman, S. and S. Pacala
2012. A forest structure model that determines crown layers and partitions growth and mortality rates for landscape-scale applications of tropical forests. *Journal of Ecology*, 100(2):508–518.

Burrascano, S., F. Lombardi, and M. Marchetti
2008. Old-growth forest structure and deadwood: Are they indicators of plant species composition? A case study from central Italy. *Plant Biosystems*, 142(2):313–323.

Burt, A., M. Disney, and K. Calders
2019. Extracting individual trees from lidar point clouds using treeseg. *Methods in Ecology and Evolution*, 10(3):438–445.

Calders, K., G. Newnham, A. Burt, S. Murphy, P. Raumonen, M. Herold, D. Culvenor, V. Avitabile, M. Disney, J. Armston, and M. Kaasalainen
2015. Nondestructive estimates of above-ground biomass using terrestrial laser scanning. *Methods in Ecology and Evolution*, 6(2):198–208.

Chave, J., D. Coomes, S. Jansen, S. L. Lewis, N. G. Swenson, and A. E. Zanne
2009. Towards a worldwide wood economics spectrum. *Ecology Letters*, 12(4):351–366.

Chehab, E. W., E. Eich, and J. Braam
2009. Thigmomorphogenesis: A complex plant response to mechano-stimulation. *Journal of Experimental Botany*, 60(1):43–56.

Chen, Y., S. J. Wright, H. C. Muller-Landau, S. P. Hubbell, Y. Wang, and S. Yu
2016. Positive effects of neighborhood complementarity on tree growth in a Neotropical forest. *Ecology*, 97(3):776–785.

Dassot, M., T. Constant, and M. Fournier
2011. The use of terrestrial LiDAR technology in forest science: application fields, benefits and challenges. *Annals of Forest Science*, 68(5):959–974.

Edelsbrunner, H. and E. P. Mucke
1994. Three-dimensional Alpha Shapes. *ACM Transactions on Graphics*, 13(1):43–72.

Everham, E. M. and N. V. L. Brokaw
1996. Forest Damage and Recovery from Catastrophic Wind. *Botanical Review*, 62(2):113–185.

Fernández-Sarría, A., L. Martínez, B. Velázquez-Martí, M. Sajdak, J. Estornell, and J. A. Recio
2013. Different methodologies for calculating crown volumes of Platanus hispanica trees using terrestrial laser scanner and a comparison with classical dendrometric measurements. *Computers and Electronics in Agriculture*, 90:176–185.

Fish, H., V. J. Lieffers, U. Silins, and R. J. Hall
2006. Crown shyness in lodgepole pine stands of varying stand height, density, and site index in the upper foothills of Alberta. *Canadian Journal of Forest Research*, 36(9):2104–2111.

Franco, M.
1986. The Influences of Neighbours on the Growth of Modular Organisms with an Example from Trees. *Philosophical Transactions of the Royal Society of London. B, Biological Sciences*, 313(1159):209–225.

Franklin, K. A. and G. C. Whitelam
2005. Phytochromes and Shade-avoidance Responses in Plants. *Annals of Botany*, 96(2):169–175.

Getzin, S., C. Dean, F. He, J. A. Trofymow, K. Wiegand, and T. Wiegand
2006. Spatial patterns and competition of tree species in a Douglas-fir chronosequence on Vancouver Island. *Ecography*, 29(5):671–682.

Gilbert, I. R., G. P. Shavers, P. G. Jarvis, and H. Smith
1995. Photomorphogenesis and canopy dynamics. Phytochrome-mediated proximity perception accounts for the growth dynamics of canopies of Populus trichocarpa x deltoides 'Beaupre'. *Plant, Cell and Environment*, 18(5):475–497.

Gonzalez de Tanago, J., A. Lau, H. Bartholomeus, M. Herold, V. Avitabile, P. Raumonen, C. Martius, R. C. Goodman, M. Disney, S. Manuri, A. Burt, and K. Calders
2018. Estimation of above-ground biomass of large tropical trees with terrestrial LiDAR. *Methods in Ecology and Evolution*, 9(2):223–234.

Goudie, J. W., K. R. Polsson, and P. K. Ott
2009. An empirical model of crown shyness for lodgepole pine (Pinus contorta var. latifolia [Engl.] Critch.) in British Columbia. *Forest Ecology and Management*, 257(1):321–331.

Grams, T. E. E. and C. P. Andersen
2007. Competition for resources in trees: physiological versus morphological plasticity. *Progress in botany*, Pp. 356–381.

Halpern, C. and T. Spies
2008. Plant Species Diversity in Natural and Managed Forests of the Pacific Northwest. *Ecological Applications*, 5(4):913–934.

Hardiman, B. S., G. Bohrer, C. M. Gough, C. S. Vogel, and P. S. Curtis
2011. The role of canopy structural complexity in wood net primary production of a maturing northern deciduous forest. *Ecology*, 92(9):1818–1827.

Hardiman, B. S., C. M. Gough, A. Halperin, K. L. Hofmeister, L. E. Nave, G. Bohrer, and P. S. Curtis
2013. Maintaining high rates of carbon storage in old forests: A mechanism linking canopy structure to forest function. *Forest Ecology and Management*, 298:111–119.

Hossain, S. M. Y. and J. P. Caspersen
2012. In-situ measurement of twig dieback and regrowth in mature Acer saccharum trees. *Forest Ecology and Management*, 270:183–188.

Ishii, H. and S. Asano
2010. The role of crown architecture, leaf phenology and photosynthetic activity in promoting complementary use of light among coexisting species in temperate forests. *Ecological Research*, 25(4):715–722.

Ishii, H. T., S. Tanabe, and T. Hiura
2004. Exploring the Relationships Among Canopy Structure, Stand Productivity, and Biodiversity of Temperate Forest Ecosystems. *Forest Science*, 50(3):342–355.

Itakura, K. and F. Hosoi
2018. Automatic individual tree detection and canopy segmentation from three-dimensional point cloud images obtained from ground-based lidar. *Journal of Agricultural Meteorology*, 74(3):109–113.

Jaffe, M. J., A. H. Wakefield, F. Telewski, E. Gulley, and R. Biro
1985. Computer-assisted image analysis of plant growth, thigmomorphogenesis and gravitropism. *Plant physiology*, 77:722–730.

Jucker, T., O. Bouriaud, and D. A. Coomes
2015. Crown plasticity enables trees to optimize canopy packing in mixed-species forests. *Functional Ecology*, 29(8):1078–1086.

Korhonen, L., J. Vauhkonen, A. Virolainen, A. Hovi, and I. Korpela
2013. Estimation of tree crown volume from airborne lidar data using computational geometry. *International Journal of Remote Sensing*, 34(20):7236–7248.

Krajicek, J., B. Kennet, and S. Gingrich
1961. Crown Competition - A measure of Diversity. *Science*, 7(1):35–42.

Lafarge, T., B. Pateiro-López, A. Possolo, and J. P. Dunkers
2014. R Implementation of a Polyhedral Approximation to a 3D Set of Points Using the α -Shape. *Journal of Statistical Software*, 56(4).

Lau, A., L. P. Bentley, C. Martius, A. Shenkin, H. Bartholomeus, P. Raumonen, Y. Malhi, T. Jackson, and M. Herold
2018. Quantifying branch architecture of tropical trees using terrestrial LiDAR and 3D modelling. *Trees - Structure and Function*, 32(5):1219–1231.

Lau, A., K. Calders, H. Bartholomeus, C. Martius, P. Raumonen, M. Herold, M. Vicari, H. Sukhdeo, J. Singh, and R. C. Goodman
2019. Tree biomass equations from terrestrial LiDAR: A case study in Guyana. *Forests*, 10(6):1–18.

Lawrence, M. C. and P. M. Colman
1993. Shape Complementarity at Protein/Protein interfaces. *Journal of Molecular Biology*, 234(4):946–950.

Lecigne, B., S. Delagrange, and C. Messier
2018. Exploring trees in three dimensions: VoxR, a novel voxel-based R package dedicated to analysing the complex arrangement of tree crowns. *Annals of Botany*, 121(4):589–601.

Lewis, M. and J. D. Murray
1993. Modelling territoriality and wolf–deer interactions. *Nature*, 366(6457):738–739.

Li, J., G. Li, H. Wang, and X. Wang Deng
2011. Phytochrome Signaling Mechanisms. *The Arabidopsis Book/American Society of Plant Biologists*, 9.

Li, Y., X. Zhang, and D. Cao
2013. The Role of Shape Complementarity in the Protein-Protein Interactions. *Scientific Reports*, Pp. 3–9.

Lim, K. S.-W.
2006. Lidar remote sensing of forest canopy and stand structure. *Progress in physical geography*, 27(1):88–106.

Liu, B., H. Li, B. Zhu, R. T. Koide, D. M. Eissenstat, and D. Guo
2015. Complementarity in nutrient foraging strategies of absorptive fine roots and arbuscular mycorrhizal fungi across 14 coexisting subtropical tree species. *New Phytologist*, 208(1):125–136.

Lorimer, C. G.
1983. Tests of age-independent competition indices for individual trees in natural hardwood stands. *Forest Ecology and Management*, 6:343–360.

Malhi, Y., T. Jackson, L. Patrick Bentley, A. Lau, A. Shenkin, M. Herold, K. Calders, H. Bartholomeus, and M. I. Disney
2018. New perspectives on the ecology of tree structure and tree communities through terrestrial laser scanning. *Interface Focus*, 8(2):20170052.

Mason, N. W., F. De Bello, J. Doležal, and J. Lepš
2011. Niche overlap reveals the effects of competition, disturbance and contrasting assembly processes in experimental grassland communities. *Journal of Ecology*, 99(3):788–796.

Mason, N. W., C. Lanoiselée, D. Mouillot, J. B. Wilson, and C. Argillier
2008. Does niche overlap control relative abundance in French lacustrine fish communities? A new method incorporating functional traits. *Journal of Animal Ecology*, 77(4):661–669.

Meng, S. X., M. Rudnicki, V. J. Lieffers, D. E. B. Reid, and U. Silins
2006. Preventing crown collisions increases the crown cover and leaf area of maturing lodgepole pine. *Journal of Ecology*, 94(3):681–686.

Morin, X., L. Fahse, M. Scherer-Lorenzen, and H. Bugmann
2011. Tree species richness promotes productivity in temperate forests through strong complementarity between species. *Ecology Letters*, 14(12):1211–1219.

Muth, C. C. and F. A. Bazzaz
2003. Tree canopy displacement and neighborhood interactions. *Canadian Journal of Forest Research*, 33(7):1323–1330.

Nicholls, B. and P. A. Racey
2006. Contrasting home-range size and spatial partitioning in cryptic and sympatric pipistrelle bats. *Behavioral Ecology and Sociobiology*, 61(1):131–142.

Norel, R., S. L. Lin, H. J. Wolfson, and R. Nussinov
1994. Shape complementarity at protein–protein interfaces. *Biopolymers*, 34(7):933–940.

Palace, M., F. B. Sullivan, M. Ducey, and C. Herrick
2016. Estimating Tropical Forest Structure Using a Terrestrial Lidar. *PloS one*, 11(4):e0154115.

Peralta, G., C. M. Frost, T. A. Rand, R. K. Didham, and J. M. Tylianakis
2014. Complementarity and redundancy of interactions enhance attack rates and spatial stability in host-parasitoid food webs. *Ecology*, 95(7):1888–1896.

Petchey, O. L.
2003. Integrating methods that investigate how complementarity influences ecosystem functioning. *Oikos*, 101(2):323–330.

Pierik, R. and M. De Wit
2014. Shade avoidance: Phytochrome signalling and other aboveground neighbour detection cues. *Journal of Experimental Botany*, 65(11):2815–2824.

Poisot, T., N. Mouquet, and D. Gravel
2013. Trophic complementarity drives the biodiversity-ecosystem functioning relationship in food webs. *Ecology Letters*, 16(7):853–861.

Poorter, L., L. Bongers, and F. Bongers
2006. Architecture of 54 moist-forest tree species: traits, trade-offs, and functional groups. *Ecology*, 87(5):1289–1301.

Poorter, L., E. Lianes, M. Moreno-de las Heras, and M. A. Zavala
2012. Architecture of Iberian canopy tree species in relation to wood density, shade tolerance and climate. *Plant Ecology*, 213(5):707–722.

Pretzsch, H., P. Biber, E. Uhl, J. Dahlhausen, T. Rötzer, J. Caldentey, T. Koike, T. van Con, A. Chavanne, T. Seifert, B. d. Toit, C. Farnden, and S. Pauleit
2015. Crown size and growing space requirement of common tree species in urban centres, parks, and forests. *Urban Forestry and Urban Greening*, 14(3):466–479.

Putz, F., G. Parker, and R. Archibald
1984. Mechanical Abrasion and Intercrown Spacing. *The American Midland Naturalist*, 112(1):24–28.

Rouvinen, S. and T. Kuuluvainen
2011. Structure and asymmetry of tree crowns in relation to local competition in a natural mature Scots pine forest. *Canadian Journal of Forest Research*, 27(6):890–902.

Rudnicki, M., V. J. Lieffers, and U. Silins
2003. Stand structure governs the crown collisions of lodgepole pine. *Canadian Journal of Forest Research*, 33(7):1238–1244.

Rudnicki, M., T. H. Meyer, V. J. Lieffers, U. Silins, and V. A. Webb
2008. The periodic motion of lodgepole pine trees as affected by collisions with neighbors. *Trees - Structure and Function*, 22(4):475–482.

Rudnicki, M., U. Silins, V. J. Lieffers, and G. Josi
2001. Measure of simultaneous tree sways and estimation of crown interactions among a group of trees. *Trees - Structure and Function*, 15(2):83–90.

Ryan, K. C.
2002. Dynamic Interactions between Forest Structure and Fire Behavior in Boreal Ecosystems Silva Fennica 36(1) review articles. *Silva Fennica*, 36(1):13–39.

Schröter, M., W. Härdtle, and G. von Oheimb
2012. Crown plasticity and neighborhood interactions of European beech (Fagus sylvatica L.) in an old-growth forest. *European Journal of Forest Research*, 131(3):787–798.

Silvertown, J.
2004. Plant coexistence and the niche. *Trends in Ecology and Evolution*, 19(11):605–611.

Tang, H., M. Brolly, F. Zhao, A. H. Strahler, C. L. Schaaf, S. Ganguly, G. Zhang, and R. Dubayah
2014. Deriving and validating Leaf Area Index (LAI) at multiple spatial scales through lidar remote sensing: A case study in Sierra National Forest, CA. *Remote Sensing of Environment*, 143:131–141.

Telewski, F. W. and M. J. Jaffe
1986. Thigmomorphogenesis: Field and laboratory studies of Abies fraseri in response to wind or mechanical perturbation. *Physiologia Plantarum*, 66(2):211–218.

Tews, J., U. Brose, V. Grimm, K. Tielborger, M. Wichmann, M. Schwager, F. M Jeltsch, J. Tews, V. Grimm, K. Tielborger, M. Wichmann, M. Schwager, and F. Jeltsch
2004. Animal species diversity driven by habitat heterogeneity/diversity: the importance of keystone structures. *Journal of Biogeography*, 31:79–92.

Thorpe, H. C., R. Astrup, A. Trowbridge, and K. D. Coates
2010. Competition and tree crowns: A neighborhood analysis of three boreal tree species. *Forest Ecology and Management*, 259(8):1586–1596.

Tilman, D. and E. Snell-Rood
2014. Diversity breeds complementarity. *Nature*, 515:5–6.

Tokola, T., J. Vauhkonen, and V. Leppänen
2008. Applied 3D Texture Features in Als-Based Tree Species Segmentation. *ISPRS Conference, Georgia.*

Trucano, T. G., L. P. Swiler, T. Igusa, W. L. Oberkampf, and M. Pilch
2006. Calibration, validation, and sensitivity analysis: What's what. *Reliability Engineering and System Safety*, 91(10-11):1331–1357.

Van de Peer, T., K. Verheyen, Q. Ponette, N. N. Setiawan, and B. Muys
2018. Overyielding in young tree plantations is driven by local complementarity and selection effects related to shade tolerance. *Journal of Ecology*, 106(3):1096–1105.

Van Gelder, H. A., L. Poorter, and F. J. Sterck
2006. Wood mechanics, allometry, and life-history variation in a tropical rain forest tree community. *New Phytologist*, 171(2):367–378.

Vauhkonen, J., T. Tokola, P. Packalén, and M. Maltamo
2009. Identification of scandinavian commercial species of individual trees from airborne laser scanning data using alpha shape metrics. *Forest Science*, 55(1):37–47.

Venjakob, C., A. M. Klein, A. Ebeling, T. Tscharntke, and C. Scherber
2016. Plant diversity increases spatio-temporal niche complementarity in plant-pollinator interactions. *Ecology and Evolution*, 6(8):2249–2261.

Vierling, K. T., L. A. Vierling, W. A. Gould, S. Martinuzzi, and R. M. Clawges
2008. Lidar: Shedding new light on habitat characterization and modeling. *Frontiers in Ecology and the Environment*, 6(2):90–98.

Von Gadow, K. and G. Y. Hui
2002. Characterizing forest spatial structure and diversity. *Proc. of the SUFOR international workshop: Sustainable forestry in temperate regions*, Pp. 20–30.

Vonderach, C., T. Voegtle, and P. Adler
2012. Voxel-Based Approach for Estimating Urban Tree Volume From Terrestrial Laser Scanning Data. *ISPRS - International Archives of the Photogrammetry, Remote Sensing and Spatial Information Sciences*, XXXIX-B8(September):451–456.

Watt, P. J. and D. N. Donoghue
2005. Measuring forest structure with terrestrial laser scanning. *International Journal of Remote Sensing*, 26(7):1437–1446.

West, G. B., B. J. Enquist, and J. H. Brown
2009. A general quantitative model of forest structure and dynamics. *PNAS*, Pp. 1–48.

Williams, J., C.-B. Schönlieb, T. Swinfield, J. Lee, X. Cai, L. Qie, and D. A. Coomes
2019. Three-dimensional Segmentation of Trees Through a Flexible Multi-Class Graph Cut Algorithm (MCGC). *arXiv preprint*.

Williams, L. J., A. Paquette, J. Cavender-Bares, C. Messier, and P. B. Reich
2017. Spatial complementarity in tree crowns explains overyielding in species mixtures. *Nature Ecology and Evolution*, 1(4).

Xiao, W., S. Xu, S. Oude Elberink, and G. Vosselman
2012. Change detection of trees in urban areas using multi-temporal airborne lidar point clouds. *Remote Sensing of the Ocean, Sea Ice, Coastal Waters, and Large Water Regions 2012*, 8532(0):853207.

Yan, W., H. Guan, L. Cao, Y. Yu, S. Gao, and J. Y. Lu
2018. An automated hierarchical approach for three-dimensional segmentation of single trees using UAV LiDAR data. *Remote Sensing*, 10(12).

Zheng, L. T., H. Y. Chen, and E. R. Yan
2019. Tree species diversity promotes litterfall productivity through crown complementarity in subtropical forests. *Journal of Ecology*, (January):1–10.